Measuring and modeling black carbon (BC) contamination in the SE Tibetan Plateau

**Junji Cao · Xuexi Tie · Baiqing Xu · Zhuzi Zhao ·
Chongshu Zhu · Guohui Li · Suixin Liu**

Abstract Black carbon (BC) concentrations were measured in the southeast (SE) Tibetan Plateau along the valley of the Yarlung Tsangpo River during winter (between November, 2008 and January, 2009). The measured mean concentration (0.75 μg m^{-3}) is significantly higher than the concentrations (0.004–0.34 μg m^{-3}) measured in background and remote regions of the globe, indicating that Tibetan glaciers are contaminated by BC particles in the Plateau. Because BC particles play important roles for the climate in the Tibetan Plateau, the sources and causes of the BC contamination need to be understood and investigated. In this study, a mesocale dynamical model (WRF) with BC particle modules is applied for analyzing the measurement. The analysis suggests that the major sources for the contamination in the SE Plateau were mainly from the BC emissions in eastern Indian and Bangladesh. Because of the west prevailing winds, the heavy emissions in China had no significant effects on the SE Plateau in winter. Usually, the high altitude of the Himalayas acts a physical wall, inhibiting the transport of BC particles across the mountains to the plateau. This study, however, finds that the Yarlung Tsangpo River valley causes a 'leaking wall', whereby under certain meteorological conditions, BC particles are being transported up onto the glacier. This too causes variability of BC concentrations (ranging from 0.3 to 1.5 μg m^{-3}) in a time scale of a few days. The analysis of the variability suggests that the

J. Cao · X. Tie · Z. Zhao · C. Zhu · S. Liu
SKLLQG, Institute of Earth Environment, Chinese Academy of Science, Xi'an, China

X. Tie (✉)
National Center for Atmospheric Research, Boulder, CO, USA
e-mail: xxtie@ucar.edu

B. Xu
Laboratory of Tibetan Environment Changes and Land Surface Processes, Institute of Tibetan Plateau, Chinese Academy of Science, Beijing, China

Z. Zhao
The Graduate School of Chinese Academy of Science, Xi'an, China

G. Li
Molina Center for Energy and the Environment, La Jolla, CA, USA

"leaking wall" effect cannot occur when the prevailing winds were northwest winds, during which the BC transport along the valley of the Yarlung Tsangpo River was obstructed. As a result, large variability of BC concentration was observed due to the change of prevailing wind directions.

1 Introduction

Black carbon (BC) particles are emitted from incomplete combustion of coal, diesel engines, biofuels, and biomass burning, which have important effects on atmospheric environment and climate (Warren and Wiscombe 1980; Bond et al. 2004; Jacobson 2004; Hansen and Nazarenko 2004; Li et al. 2005; McConnel et al. 2007). In recent years, the urbanization and industrialization of Asia have resulted in a rapid increase of BC emissions. Bond et al. (2007) reported that global emissions of BC increase from 1,000 Gg in 1,850 to 4,400 Gg in 2000. The emissions of BC are particularly large in China and India because of low-temperature household burning of biofuels and coal (Streets et al. 2003; Tie and Cao 2009). Because these regions are close to the Tibetan Plateau with a large amount of glaciers, the impact of BC particles on the snow and ice in Tibetan glaciers is an important issue, which needs to be better understood.

Recent studies suggest that Tibetan glaciers have been melting at an accelerating rate over the past decade, raising the threat of the shortage of water supply in the further for the surrounding countries (Xu et al. 2009; Barnett et al. 2005). Their study suggested that the deposition of BC particles plays important roles in the acceleration of the glacier melting in the Tibetan Plateau. For example, the deposition of BC on the surface of glaciers leads to the "darkening" snow and ice, producing changes in the albedo over snow and ice. Because of the high albedo of snow and ice and the albedo feedback that results with snow and ice melt, darkening of snow and ice is very effective at producing climate warming (Hansen and Nazarenko 2004; Ramanathan and Carmichael 2008). The Tibetan Plateau is a region where is very sensitive to the climate/climate changes (Flanner et al. 2007). Particularly, darkening snow in snowpack has very important impact on the heating of snow column in glacier regions (Flanner et al. 2009). Over the Tibetan Plateau, a large amount of glaciers are major water resources for the surrounding countries, such as India and China (Cao et al. 2009a; Xu et al. 2009). Thus there is an urgent need to study the BC contamination over the Tibetan Plateau.

In the past, some in-situ BC measurements had been made in the Tibetan Plateau (Cao et al. 2009b; Carrico et al. 2003). However, these measurements of BC concentrations are located in the west side of the Plateau (Cao et al. 2009b). As a result, these sites are not particularly in the region downwind of large BC sources. Engling et al. (2010) reported the ambient concentrations of black carbon at the eastern edge of the Tibetan Plateau (in Yunnan Province of China) during spring. Their measurement suggested that the BC emissions from Bangladesh, Myanmar and northeastern India had important impact on the BC contaminations at the measurement site.

In this study, we will show the BC measurements in the SE Plateau, which is surrounded by large BC source regions (such as Indian and China). Specifically, this study will address the following major concerns: (1) Where are the important BC source regions for contributing to BC contamination in the SE Plateau? (2) How are BC particles transported from the source regions to across over the Himalayas onto the SE Tibetan Plateau? The

paper is organized as follows: In Section 2, we describe the methodology of modeling and data collection. In Sections 3, we present the result and discussion.

2 Methodology of modeling and data collection

2.1 Data collection

The measurement site is located in Linzhi, Tibet (94.44^{o}E, 29.46^{o}N). The detailed information of the site and the surrounding areas are shown in Fig. 1. The site location is in the SE Tibetan Plateau and the west side of the valley of the Yarlung Tsangpo River with an altitude of 3,300 m. In the south of the site, it is the Himalaya Mountains. Around the site, there are two small villages, which are located on the east side of the site, with distances of about 30–50 km from the measurement site. Because it is in downwind regions of the site (the prevailing winds are generally west in winter), the effect of the villages on the site is minimum.

In the further south of the site, there is the region with high BC emissions (see the lower panel of Fig. 2). Because of the high altitude of the Himalayas (>5 km, see the upper panel of Fig. 2), the mountains could obstruct the transport of air pollutants from the source regions (in south of the Himalayas) to the mountains. Thus the selection of this measurement site could provide important information to better understand the causes of BC contamination over Tibetan glacier in the SE Plateau.

BC was measured continuously as 5-min averages by quartz-fiber filter tape transmission at an 880 nm wavelength with an aethalometer (Model AE-16, Magee Scientific Company, Berkley, CA, USA) (Hansen et al. 1984). The instrument was
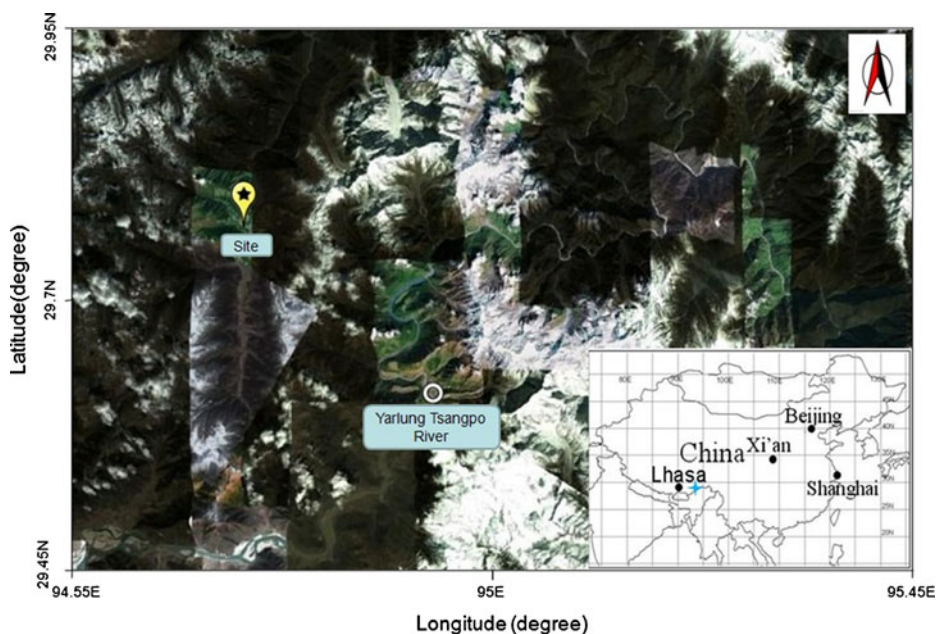

Fig. 1 The display of the measurement site, which is located in the SE Tibetan Plateau (*indicated as the black star*). The small panel in right corner indicates the measurement location in China
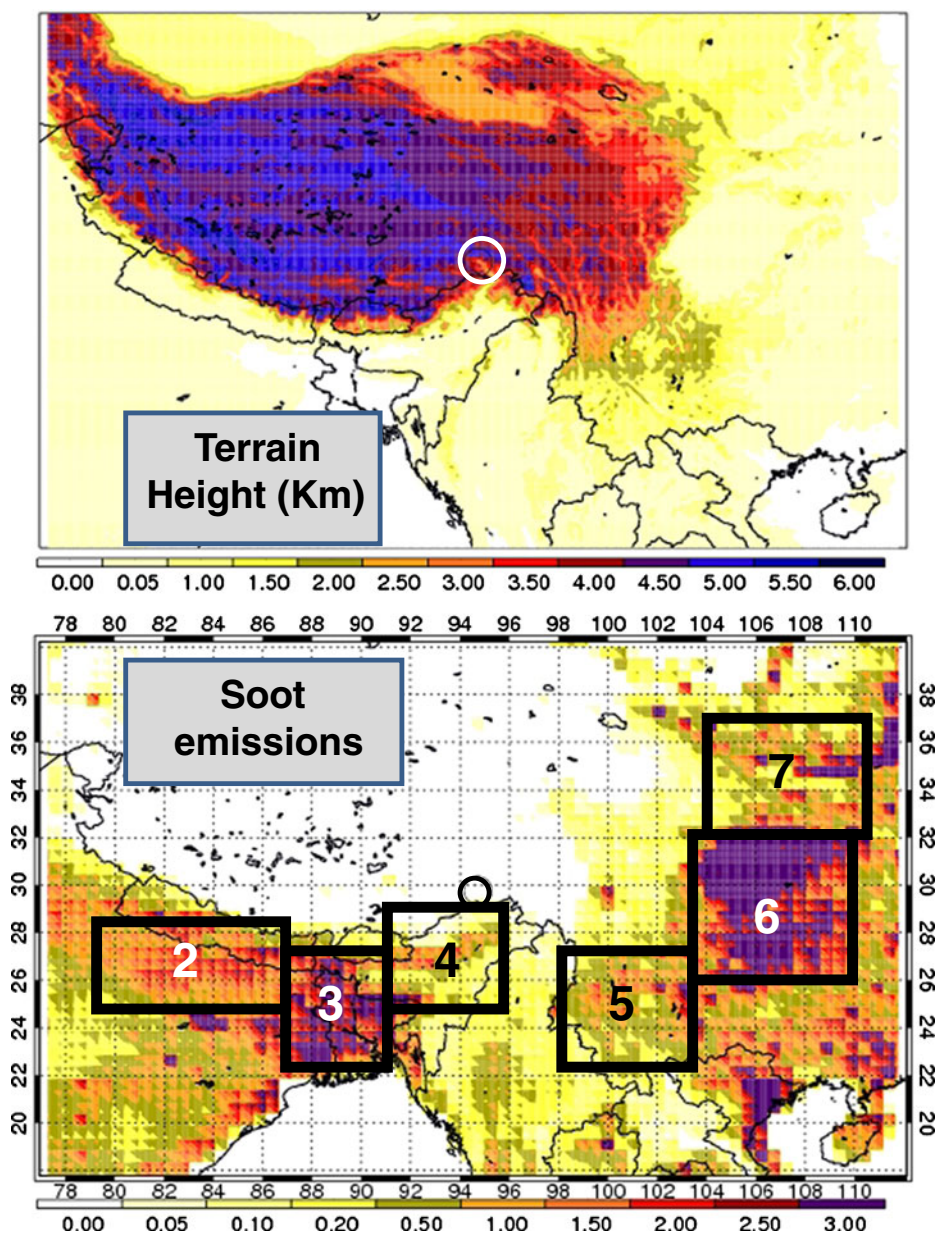
Fig. 2 The display of the model domain and the measurement site (*indicated as the white circle*) with terrain height in the Tibetan Plateau (*the upper panel*), and the soot emissions (g s^{-1}) in the vicinity of the SE Tibetan Plateau, which is used for the model simulations (*the lower panel*). The different source regions are shown by the black squares. The definition of the seven sources is shown in Table 1. The S-1 represents all BC sources in the model domain, which is not labeled in Fig. 2

placed at 2 m above ground and operated at 4 L/min. The aethelometer was connected to a TSP plastic inlet and total suspended particles (TSP) were measured. The aethalometer was factory calibrated with ±2% accuracy (Hansen et al. 1984; Allen et al. 1998). Filter

transmittance in inverse megameters (M m^{-1}) was converted to concentration in µg m^{-3} using 16,425/λ or 16.6 m^2 g^{-1} when λ=880 nm, which is the manufacturer's default derived from comparison with thermal elemental carbon (EC) measurements. This default varies by aerosol mixture (Arnott et al. 2003; Watson et al. 2005; Park et al. 2006), but the default was used in this study to retain consistency over the modeling period and with other comparison studies. The aethalometer was calibrated at least once per month.

2.2 Model methodology

To understand the sources of BC contamination on the glaciers, a high horizontal resolution dynamical model is used to study the transport pathways from BC emissions to the Plateau. In this study, a state of the art of mesoscale dynamical/ aerosol model (WRF-Chemv3; version 3) is applied to investigate the impact of BC emissions on the BC concentrations in the SE Plateau. The model includes a dynamical model (WRF) and a chemical/aerosol model (Chem). The Weather Research and Forecasting (WRF) model is a mesocale numerical weather prediction system designed to serve both operational forecasting and atmospheric research needs. The WRF model is a fully compressible and Euler nonhydrostatic model. The Yonsei University PBL scheme is used for calculating PBL height in this study. The detailed description of WRF model was given by Grell et al. (2005).

In this study, the model is simplified to fit the need of the study. The complicated chemical schemes of gaseous and aerosols are reduced, and only the modules (emission, transport, and deposition) related to the calculation of BC particles are remained in this study. The model resolution is selected to being 9 km in a 4,500× 3,600 km domain centered on the SE Tibetan Plateau (see the upper panel of Fig. 2). The relatively high horizontal resolution (9 km) is necessary for simulating the meteorological conditions in the complicated topography of the Tibetan Plateau. The BC emission inventory used in this study was constructed by Streets et al. (2003) with a 0.5×0.5° resolution, and was linearly interpolated to the model resolution. The model runs from Jan. 1 to Jan. 30, 2009 for studying the BC distributions during winter season when the area of Tibetan glacier reaches its maximum. The initial and boundary conditions are constrained by the National Center for Environmental Prediction (NCEP) winds with every 6-hour interval, and the time step of the model simulation is 90 s. Because the dynamical and aerosol modules are coupled in an on-line mode, high temporal variations of meteorology and aerosol are resolved in the model simulations.

In order to assess the BC sources, which have important impacts on the elevated BC concentrations measured in the SE Plateau, seven different BC sources (based on their geographical locations) are defined in the model study (as highlighted in the lower panel of Fig. 2). The definition of the seven sources is described in Table 1. In the model simulations, seven different BC tracers are included in the model to correspond the 7 BC sources. As a result, the relative contribution of the 7 BC sources can be calculated in the model. The source 1 (S-1) represents the total BC emission sources in the model domain. Other six sources, as indicated in Fig. 2, are either in southern or eastern regions of the Plateau with high BC emissions. Thus, with a favorable wind condition, any these sources could have important effects on the BC contaminations of the glaciers. In this study, the individual contribution of the seven sources to the contamination of the SE Plateau is assessed by the WRF-Chemv3 model, and the results show in the following sections.

Table 1 The definition of seven different BC sources used in the sensitivity study of the model

Source definition	Source description
S-1	All BC emissions in the model domain
S-2	BC source located in the west part of India
S-3	BC source located in the middle part of India and Bangladesh
S-4	BC source located in the east part of India
S-5	BC source located in Yuan Province of China
S-6	BC source located in Sichuan Province of China
S-7	BC source located in Shaanxi Province of China

3 Results and analysis

3.1 Characteristics of measured BC concentrations

The measurement of BC concentrations in winter between Nov. 2008 and Jan. 2009 is presented and analyzed. Figure 3 shows the temporal variation of the measured BC concentrations. The uncertainty bars represent one standard deviation in Fig. 3. It shows that there was a large daily variability of the concentrations, with a minimum of 0.3 μg m^{-3} and a maximum of 1.6 μg m^{-3}, respectively. This large daily variability suggested that mesoscale meteorological variations have important impacts on the BC concentrations at the measurement site. Despite of the large daily variation, there was very small variability for the monthly averaged concentrations. For example, the monthly averaged concentrations were 0.75±0.17, 0.65±0.16, and 0.75±0.34 μg m^{-3} in Nov. 2008, Dec. 2008, and Jan. 2009,
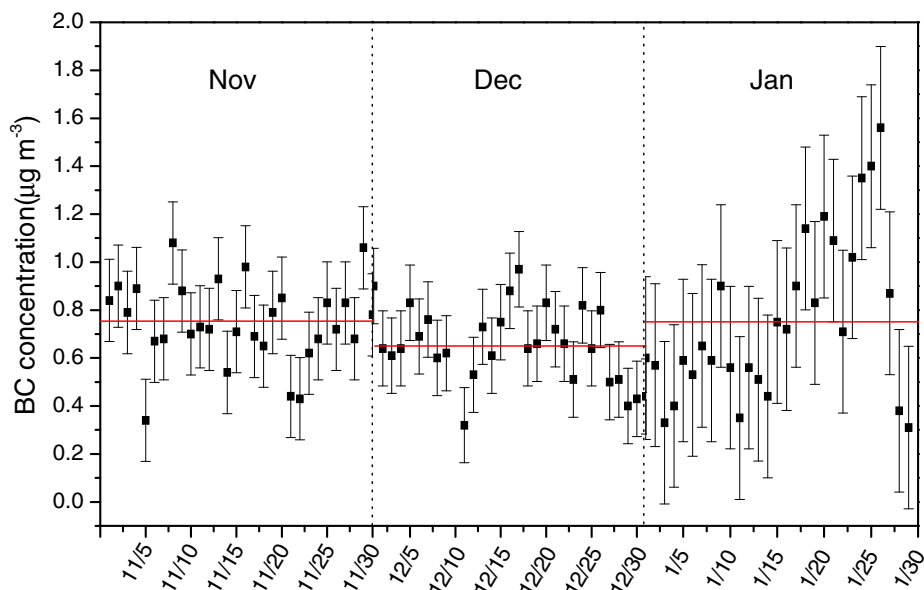

Fig. 3 The measured daily averaged BC concentrations (μg m^{-3}) between November, 2008 and January, 2009. The red lines show the monthly averaged concentrations. The uncertainty bars represent one standard deviation

respectively, suggesting that the averaged concentration (0.74 µg m^{-3}) during winter was relatively high with slight variation during each month.

Table 2 shows the comparison of the measured mean concentration with other measurements in various locations (background, remote, small-medium cities, and large cities) across the globe. The highlight points of the comparison are as follows: (1) The measured mean concentration is significantly higher than the background value (0.0035 µg m^{-3}) measured in the Antarctic region. (2) The measured mean concentration is considerably higher than the value in the remote regions (0.29–0.34 µg m^{-3}) around the globe. (3) The measured mean concentration is lower than the values measured in cities (small, median, and large) in different continents. Because the measurement site is located in a remote area and no major BC emissions are located in the vicinity of the measurement site (see Fig. 1), the long-range transport from the surrounding BC sources to the Plateau is the major cause for the elevated BC concentrations. Thus, it is important to understand the sources and the transport pathways of the BC contamination on the SE Plateau.

3.2 The sources of BC contamination

Figure 4 shows the calculated BC concentrations in the Tibetan Plateau attributed to the 7 BC sources. The calculation shows that the BC concentrations are considerably high (~15 µg m^{-3}) in the surrounding areas of the Tibetan Plateau, especially in the

Table 2 Comparison average BC concentrations for different locations

| Locations	Site reorientations	Sampling date	Concentrations (µg m-3)	References
Southeast Tibet	Mountain Glacier	2009.1	0.76	This work
Southeast Tibet	Mountain site	2004.4–5	1.47	Engling et al. 2010
Mutztagh, West Tibet	Mountain Glacier	2003.12–2006.02	0.055	Cao et al. 2009a
Wailiguan, China	Remote	1994.7–1995	0.13–0.3	Tang et al. 1999
St Dennis, England	Remote	1996.11	0.508	Bhugwant et al. 2000
Halley, South Pole	Back ground	1992–1995	0.001	Wolff and Cachier 1998
South Pole	Back ground	1992–1995	0.006	Wolff and Cachier 1998
Xi'an, China	Large City	2003.9–2005.8	14.7	Cao et al. 2009b
Guanzhou, China	Large City	2003.1	14.5	Cao et al. 2007
Beijing, China	Large City	2003.1	7.1	Cao et al. 2007
Shanghai, China	Large City	2003.1	8.3	Cao et al. 2007
Pune, India	Large City	2005.1–2005.12	4.1	Safai et al. 2007
Bangalore, India	Large City	2001.11	4.2	Babu and Moorthy 2002
Kanpur, India	Large City	2004.12	6.0–20.0	Tripathi et al. 2005
Paris, France	Large City	1997.8–1997.10	14±7	Ruellan, and Cachier 2001
Zurich, Switzerland	Median City	1998.1–1999.3	1.7	Putaud, et al. 2004
Bologna, Italy	Median City	2000.1–2000.12	2.9	Putaud, et al. 2004
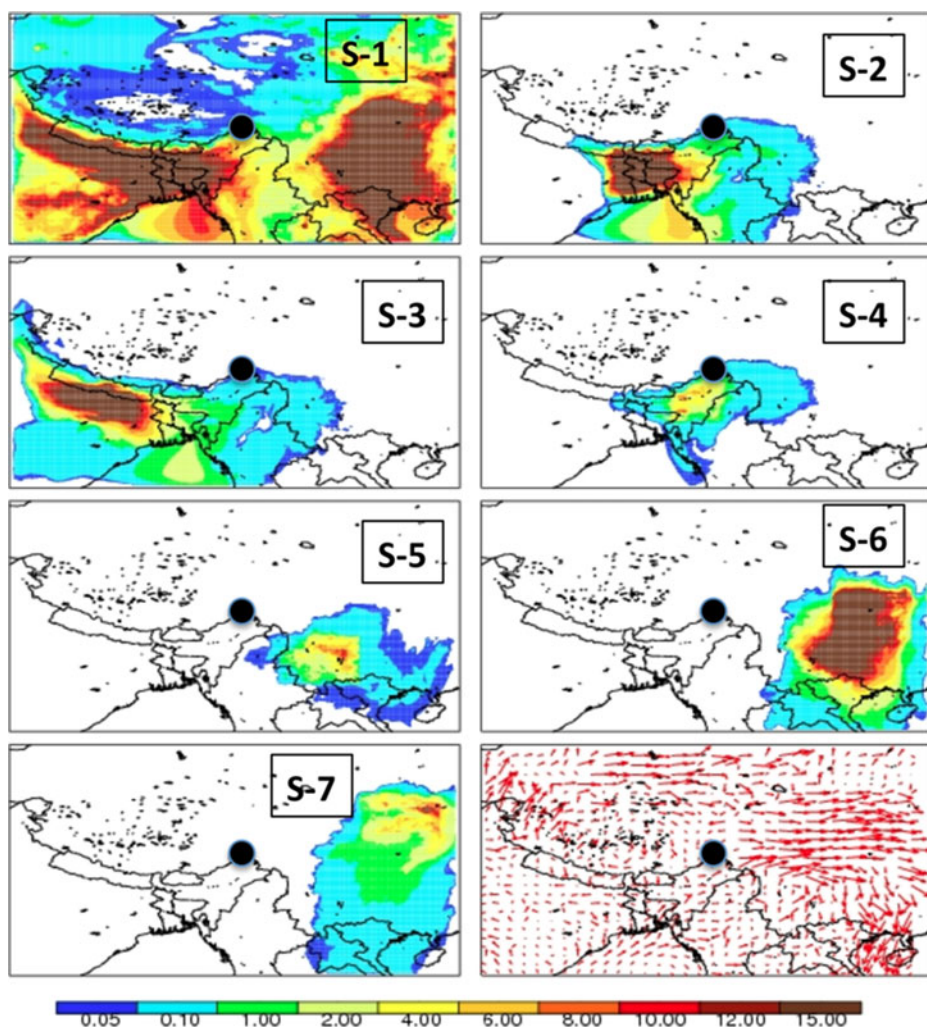
Fig. 4 The model calculated BC concentrations ($\mu g\ m^{-3}$) averaged in January, 2009 due to the 7 BC sources. The panel eight shows the averaged wind distribution

south of Himalaya Mountains and in Sichuan Province of China. There is also a strong horizontal gradient of BC concentrations along the Himalaya Mountains, indicating that the Himalaya Mountains obstruct the transport of BC from the south to the north of the Himalaya Mountains. Figure 5 shows a detailed illustration of the BC obstruction by the Himalaya Mountains. The calculation suggests that BC particles are strongly obstructed by the Himalayas, and the elevated mountains act as a "physical wall" to resist the BC to across from the top of mountains. However, we note that there are some filaments of BC concentrations in the Plateau, suggesting the occurrence of BC contamination in the Plateau.

Although the BC concentrations over the Plateau are low (shown in Figs. 4 and 5), the BC contamination in the Plateau is also noticeable. For example, as indicated by the cases of S-1, S-2, S-3, and S-4, BC particles penetrate from the south Himalayas
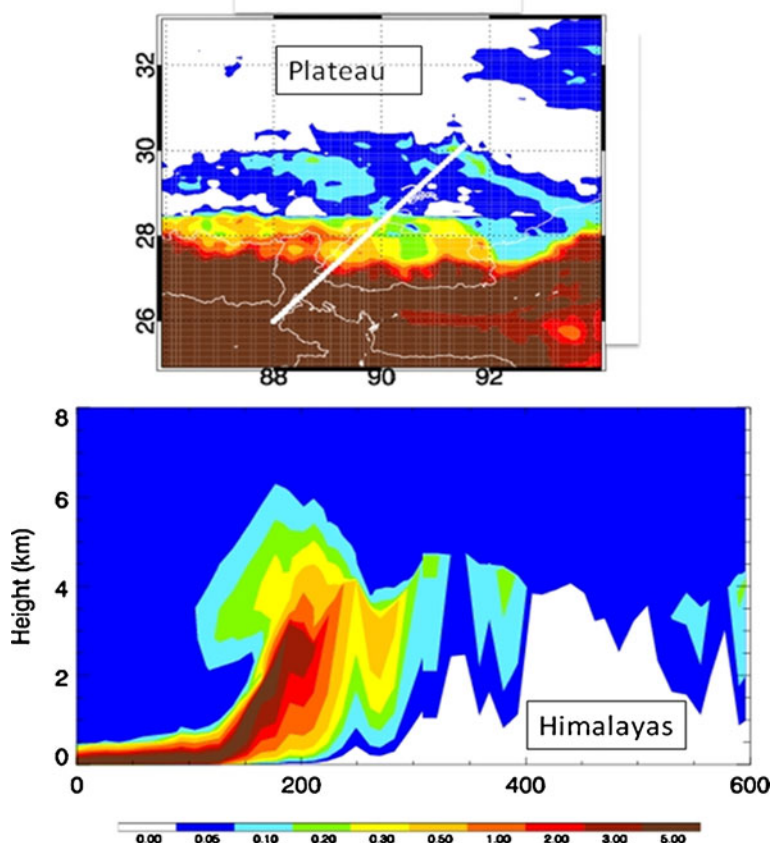
Fig. 5 The model calculated surface distribution of BC concentrations ($\mu g\ m^{-3}$) (*the upper panel*), and the cross section of BC along a pathway (*lower panel*) indicated by the white line in the upper panel

to the Plateau. In addition, the calculation suggests that S-4 (east Indian source) has maximum effect on the BC contamination in the SE Plateau, following by S-3 and S-2 (see also Fig. 4). In contrast, S-5, S-6, and S-7 have no clearly impacts on the BC contaminations in the Plateau, due to the fact that the prevailing winds were normally west or northwest winds during winter (see the last panel of Fig. 4).

3.3 The cause of BC contamination in SE Tibetan Plateau

From the above analysis, we show the evidence that the BC emissions in the south Himalayas have important impacts on the BC contaminations in the Plateau. Figure 5 illustrates the BC penetration from the Himalayas to the Plateau. Figure 5 shows that in a particular case, the calculated horizontal distribution of BC has a strong horizontal gradient. For example, in the south of 28°N, the BC concentrations are very high, while in the north of 28°N, the BC concentrations are very low (as shown in the upper panel of Fig. 5). In the lower panel of Fig. 5, it shows the calculated cross section of BC concentrations along the white line of the upper panel. The result suggests that the Himalayas obstruct BC particles to be transported across the Plateau. However, this obstruction is not completed, and some residual BC particles are transported across the Himalayas. Thus, an important question

needs to be addressed, i.e., how are the BC particles transported from the source regions in the south Himalayas to across over the "wall" to reach the Plateau?

Figure 6 shows the frequency distribution of the measured BC concentrations between Nov. 2008 and Jan. 2009. It shows the occurrence frequencies at different BC concentrations. The result suggests that the highest frequency occurred at the concentration of 0.38 μg m^{-3}, which was considerably smaller than the averaged concentration of 0.75 μg m^{-3}. However, there was a long tail, in which it contained low frequencies and high concentrations. For example, at the concentration of 1.0 μg m^{-3}, the frequency was about 10, while at the concentrations of 2.0–6.0 μg m^{-3}, the frequency decreased to less than 5. The total frequency for the concentrations (>0.75 μg m^{-3}) occurred only 28%. In contrast, the concentrations (<0.75 μg m^{-3}) occurred 72%. This result suggests that the high concentrations of BC from the high emission regions can occasionally across the Himalayas to cause the contaminations in the Plateau.

Figure 7 shows the comparison between the calculated and measured BC concentrations in the measurement site in January, 2009, when the measured temporal variation was highest. The result indicates that the calculated BC concentrations tend to underestimate the measured values. For example, the calculated mean concentration is 0.66 μg m^{-3}, which is about 13% smaller than the measured mean concentration of 0.75 μg m^{-3}. Figure 7 also further indicates that the contribution from the S-4 source to the BC concentrations at the measurement site is highest, suggesting that the BC emissions in east Indian have important effects on the BC contamination in the SE Plateau. Despite the underestimation by the model, there is a similarity between the calculated and measured BC concentrations, especially for their temporal variations. For example, there were three measured peaks on Jan. 9, Jan. 18–21, and Jan. 25–27, respectively. As mentioned above, these peaks caused the high BC concentrations in
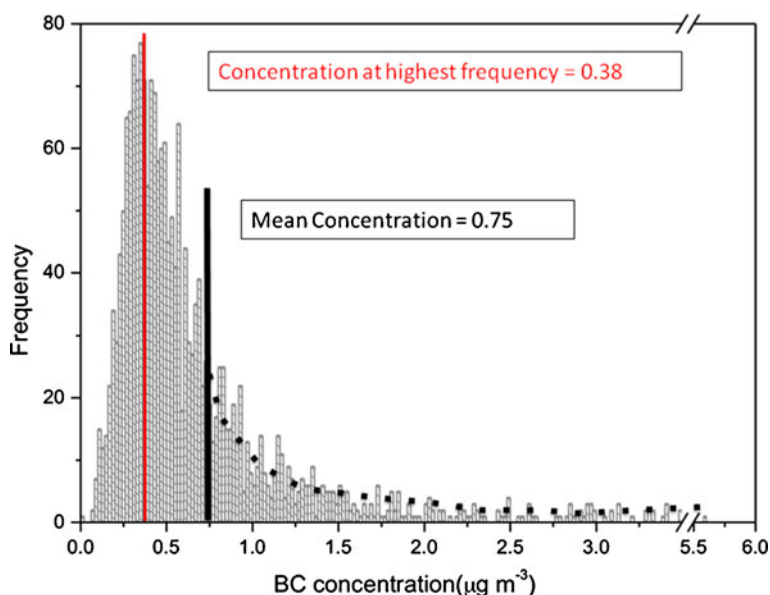

Fig. 6 The measured occurrence frequency at different BC concentrations. The red line represents the concentration at the highest occurrence, and the black line represents the mean concentration during the measurement period
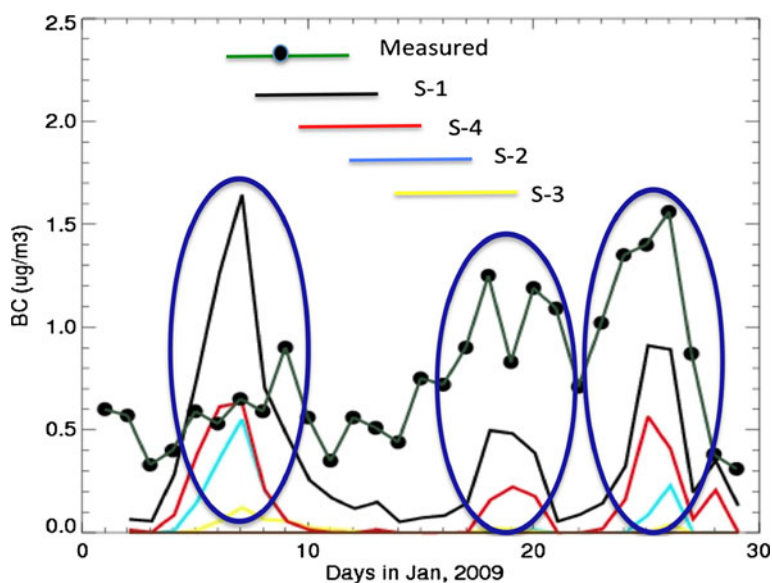
Fig. 7 The calculated (*lines*) and measured (*dot-line*) BC temporal variability at the measurement site during January, 2009. The black, blue, yellow, and red lines represents the BC concentrations (μg/m³) due to the S-1, S-2, S-3, and S-4 BC sources, respectively

the Plateau. For example, the averaged peak value in January was 1.18 μg m⁻³, while the non-peak period was 0.56 μg m⁻³. Thus, understanding the formation of BC episodes is the key to study the BC contamination in the SE Plateau. Similar to the measurement, the calculation also shows a strong BC episodes, but with some differences compared to the measured result. For example, in the calculation, there are also three BC peaks, which is consistent with the measurements, but with some discrepancies. The calculated peak on Jan. 9 is overestimated the measured value, and is about 1 day ahead of the measured peak. For the peaks on Jan. 18–21, and Jan. 25–27, the model calculation shows a similar timing to the measured peaks, but the peak values are smaller than the measured peaks.

In the model, because the BC emissions have no day-day variation, the strong BC episodes in a short period (days) are mainly resulted from mesoscale meteorological variations as suggested by several previous studies (Tie et al. 2009; Bei et al. 2010; de Foy et al. 2008). In order to understand the effect of the mesoscale meteorology on the BC episodes, Fig. 8 shows the detailed wind (speeds and directions) distribution and the calculated BC distribution in the vicinity of the measurement site. The upper and lower panels show the wind and BC distributions during both the non-peak (Jan. 13) and the peak (Jan. 25) periods. During the peak period (lower panel), the prevailing winds were strong west winds, and there was a transport pathway along the valley of the Yarlung Tsangpo River, generating a northwest "valley wind" and allowing BC particles to be transported from the heavily polluted regions to the uphill of the Himalayas. After BC particles reached to the Plateau, the strong west winds were merged with the northwest "valley wind", transporting BC particles toward to NWW (northwest-west) direction and resulting in the BC contamination in the SE Plateau (see lower panel of Fig. 8). On Jan. 18 (another measured high BC episode), the "valley wind" and the same valley transport pathway were also occurred (not
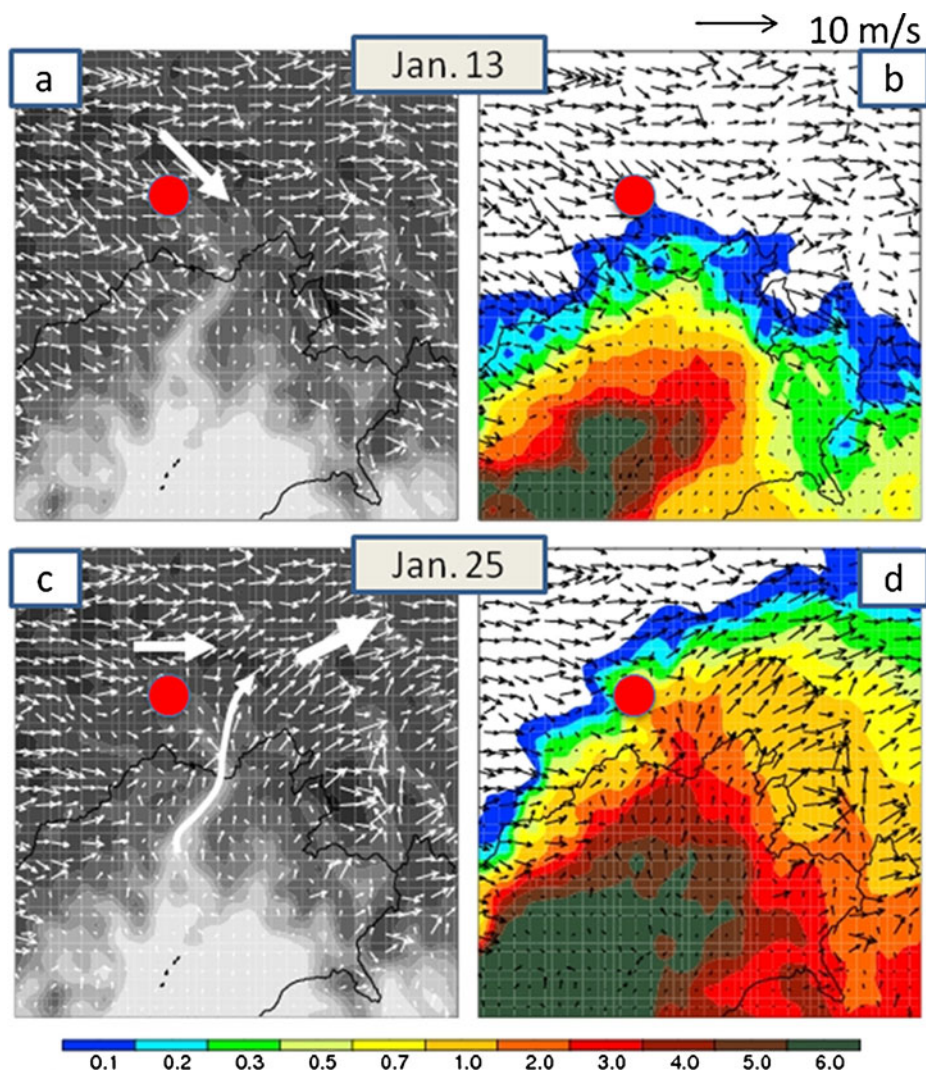
Fig. 8 Detailed wind patterns (*left panels*) and the corresponding BC distributions (*right panels*) calculated by the model. The upper panels display the case that when measured BC concentration was low (Jan/13, 2009), while the lower panels display the case that when measured BC concentration was high (Jan/25, 2009). In the left panels, the white-black represent the terrain heights (*white is low and black is high*)

shown). In contrast, on Jan. 13, when the measured BC was in the non-peak period, the prevailing winds in the vicinity of the measurement site were southwest winds. The southwest winds obstructed the transport pathway along the valley of the Yarlung Tsangpo River, and the "valley wind" cannot occur. As a result, there was no significant transport of BC particles from the source regions to the SE Plateau, causing a lower BC concentration on this day.

In order to obtain a statistical result of the "valley wind", two different events are classified and analyzed, i.e., the low and high BC events in the measurement. As shown in Fig. 7, there were several maxima and minima. For example, on 18, 20, 25, and 26th of

January, maximum of BC concentrations occurred, which is classified as the high BC events. In contrast, on 11, 13, 22, and 28th of January, minimum of BC concentrations occurred, which is classified as the low BC event. In Fig. 9, the averaged winds and BC concentrations are calculated for the two situations. As shown in Fig. 9, in the low BC events (the upper panels), the prevailing winds were generally southwestward. For example, in the area of 93–94°E and 29.5–30°N, the averaged wind direction was NW with a mean speed of 1.6 m/s. As we mentioned in the case study (shown in Fig. 8), the NW winds obstructed the "valley wind", which prevented the BC contamination. In contrast, in the high BC event (the lower panels), the averaged wind direction in
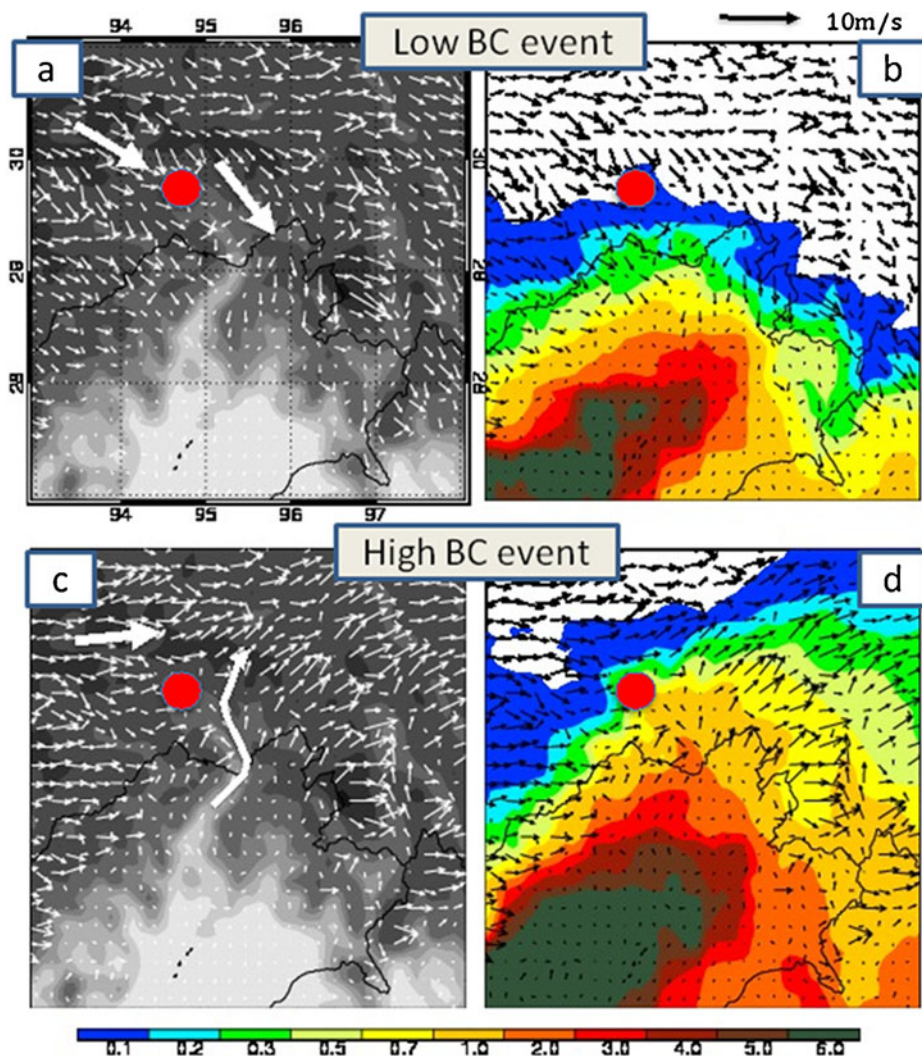

Fig. 9 Averaged winds and BC concentrations in two different events, i.e., the low and high BC events in the measurement. In the low BC event (*the upper panels*), the result is averaged condition on 11, 13, 22, and 28th of January. In the high BC event (*the lower panels*), the result is averaged conditions on 18, 20, 25, and 26th of January

the area of 93–94°E and 29.5–30°N was SWW, with a mean speed of 2.3 m/s. In this case, the "valley wind" occurred, and BC concentrations were elevated at the measurement site (~0.7 gm^{-3}).

Based on the above analysis, the valley of the Yarlung Tsangpo River plays important rules to transport BC particles from the source regions to across the "wall" of the Himalayas to reach the Plateau, causing the BC contaminations in the region. Thus, the valley of the Yarlung Tsangpo River can be considered as a "leaking wall" of the Himalayas. This "leaking wall" effect could produce very important impacts on the ecosystem in the Tibetan Plateau, such as the changes in glaciers over the Tibetan Plateau. However, this issue is out of the focus of this study, and needs to be carefully investigated. In addition, this analysis also suggests that the transport of BC particles from the source regions through the "valley wind" is strongly dependent upon the direction of prevailing winds. When the prevailing winds are west winds, it is favorable for the occurrence of the "valley wind", causing high BC concentrations in the SE Plateau. In contrast, when the prevailing winds are northwest winds, the "valley wind" is obstructed by the prevailing winds, resulting in low BC concentrations. As a result, the changes of prevailing winds (from west to northwest) produce a large variability of BC concentrations in the vicinity of the SE Tibetan Plateau.

4 Summary

The Tibetan Plateau is covered by a large amount of glaciers, which are major water resources for the surrounding countries. Recent studies suggest that Tibetan glaciers have been melting at an accelerating rate over the past decade, raising the threat of the shortage of water supply in the further for the surrounding countries. One of the reasons of the melting snow is caused by the contamination of BC particles on snow. For example, the deposition of BC on the surface of glaciers tends to "darkening" snow, producing changes in snow albedo and the enhancement of the absorption of solar radiation on snow. Thus, in-situ measurement of BC concentration in the Tibetan Plateau is urgently needed to better understand the "darkening" snow effect over Tibetan glaciers.

In this study, we present the measurement of black carbon (BC) in the southeast (SE) Tibetan Plateau during winter, 2009. The result shows that the mean concentration (0.75 μg m^{-3}) is significantly higher than the concentrations measured in background and remote regions (0.004–0.34 μg m^{-3}) in the globe, indicating that Tibetan glacier is contaminated by BC particles in the SE Tibetan Plateau. In order to analyze the sources and the causes of the BC contaminations over the glacier in the SE Plateau, a mesoscale dynamical model (WRF) with the modules of BC particles is applied for this study. In the model simulation, the individual contribution of BC sources from different regions in the vicinity of the SE Plateau (such as BC emissions from Indian, Bangladesh, and China) to the BC concentrations is analyzed. The analysis suggests that the major sources for the BC contaminations in the SE Plateau are mainly from the emissions in eastern Indian and Bangladesh. Because of the west prevailing winds, the heavy BC emissions in China have no significant effects on the measured BC contamination in the SE Plateau in winter.

The model simulation is also applied to analyze the causes of the measured high BC episodes, which significantly contribute to the BC contaminations in the Plateau. The

analysis suggests that during high BC episodes, BC particles from the source regions were transported along the valley of the Yarlung Tsangpo River to the uphill of the Himalayas, causing the high BC concentrations in the SE Plateau. Because of the high altitude, the Himalayas act as a "physical wall" to obstruct BC particles to across over the mountains. Thus, the BC transport along the valley of the Yarlung Tsangpo River can be considered as a "leaking wall", which is the main cause for the BC contaminations in the SE Plateau. The effect of the "leaking wall" is an important funding of this study, which leads to better understanding the air pollutants to transport across over the Himalayas. Further analysis shows that meteorological conditions have important impacts on the "leaking wall" effect. When the prevailing winds are west winds, it is favorable for the occurrence of the "valley wind", causing the high BC concentrations in the Plateau. In contrast, when the prevailing winds are northwest winds, the "valley winds" is obstructed by the prevailing winds, resulting in low BC concentrations. As a result, the changes of the prevailing winds (from west to northwest) produce a large variation of BC concentrations in the vicinity of the SE Tibetan Plateau.

References

Allen, G.A., Lawrence, J., Koutrakis, P.: Field validation of a semi-continuous method for aerosol black carbon (aethalometer) and temporal patterns of summertime hourly black carbon measurements in southwestern PA. Atmos. Environ. **33**, 817–823 (1998)

Arnott, W.P., Moosmuller, H., Sheridan, P.J., Ogren, J.A., Raspet, R., Slaton, W.V., Hand, J.L., Kreidenweis, S.M., Collett Jr., J.L.: Photoacoustic and filter-based ambient aerosol light absorption measurements: instrument comparisons and the role of relative humidity. J. Geophys. Res. **108**, 4034 (2003). doi:10.1029/2002JD002165

Babu, S.S., Moorthy, K.K.: Aerosol black carbon over a tropical coastal station in India. Geophys. Res. Lett. **29**(23), 2098 (2002). doi:10.1029/2002GL015662

Barnett, T.P., Adam, J.C., Lettenmaier, D.P.: Potential impacts of a warming climate on water availability in snow-dominated regions. Nature **438**, 303–309 (2005)

Bei, N., Lei, W., Zavala, M., Molina, L.T.: Ozone predictabilities due to meteorological uncertainties in the Mexico City basin using ensemble forecasts. Atmos. Chem. Phys. **10**, 6295–6309 (2010). doi:10.5194/acp-10-6295-2010

Bhugwant, C., Cachier, H., Bessafi, H., Leveau, J.: Impact of traffic on black carbon aerosol concentration at la ReH union Island (Southern Indian Ocean). Atmos. Environ. **34**, 3463–3473 (2000)

Bond, T., Streets, D.G., Yarber, F.Y.K.F., Nelson, S.M., Woo, J.H., Klimont, Z.: A technology-based global inventory of black and organic carbon emissions from combustion. J. Geophys. Res. **109**, D14203 (2004). doi:10.1029/2003JD003697

Bond, T.C., Bhardwaj, E., Dong, R., Jogani, R., Jung, S., Roden, C., Streets, D.G., Trautmann, N.M.: Historical emissions of black and organic carbon aerosol from energy-related combustion, 1850–2000. Global Biogeochem. Cy. **21**, GB2018 (2007). doi:10.1029/2006GB002840

Cao, J.J., Lee, S.C., Chow, J.C., Watson, J.G., Ho, K.F., Zhang, R.J., Jin, Z.D., Shen, Z.X., Chen, G.C., Kang, Y.M., Zou, S.C., Zhang, L.Z., Qi, S.H., Dai, M.H., Cheng, Y., Hu, K.: Spatial and seasonal distributions of carbonaceous aerosols over China. J. Geophys. Res. **112**, D22S11 (2007). doi:10.1029/2006JD008205

Cao, J.J., Xu, B.Q., He, J.Q., Liu, X.Q., Han, Y.M., Wang, G.H., Zhu, C.S.: Concentrations, seasonal variations, and transport of carbonaceous aerosols at a remote mountainous region in western China. Atmos. Environ. **43**, 4444–4452 (2009a)

Cao, J.J., Zhu, C.S., Chow, J.C., Watson, J.G., Han, Y.M., Wang, G.H., Shen, Z.X., An, Z.S.: Black carbon relationships with emissions and meteorology in Xi'an. Chin. Atmos. Res. **94**, 194–202 (2009b)

Carrico, C.M., Bergin, M.H., Shrestha, A.B., Dibb, J.E., Gomes, L., Harris, J.M.: The importance of carbon and mineral dust to seasonal aerosol properties in the Nepal Himalaya. Atmos. Environ. **37** (20), 2811–2824 (2003)

de Foy, B., Fast, J.D., Paech, S.J., Phillips, D., Walters, J.T., Coulter, R.L., Martin, T.J., Pekour, M.S., Shaw, W.J., Kastendeuch, P.P., Marley, N.A., Retama, A., MolinaBasin-scale, L.T.: Wind transport during the MILAGRO field campaign and comparison to climatology using cluster analysis. Atmos. Chem. Phys. **8**, 1209–1224 (2008)

Engling, G., Zhang, Y.N., Chan, C.Y., Sang, X.F., Lin, M., Ho, K.F., Li, Y.S., Lin, C.Y., Lee, J.J.: Characterization and sources of aerosol particles over the Southeastern Tibetan Plateau during the Southeast Asia biomass-burning season. Tellus (2010). doi:10.1111/j.1600-0889.2010.00512

Flanner, M.G., Zender, C.S., Randerson, J.T., Rasch, P.J.: Present-day climate forcing and response from black carbon in snow. J. Geophys. Res. **112** (2007). doi:10.1029/2006JD008003

Flanner, M.G., et al.: Springtime warming and reduced snow cover from carbonaceous particles. Atmos. Chem. Phys. **9**, 2481–2497 (2009)

Grell, G.A., Peckham, S.E., Schmitz, R., McKeen, S.A., Wilczak, J., Eder, B.: Fully coupled "online" chemistry within the WRF model. Atmos. Environ. **39**, 6957–6975 (2005)

Hansen, A., Rosen, H., Novakov, T.: The aethalometer—An instrument for the real-time "measurement of optical absorption by aerosol particles. Sci. Total Environ. **36**, 191–196 (1984)

Hansen, J., Nazarenko, L.: Soot climate forcing via snow and ice albedos. PNAS **101**, 423–428 (2004)

Jacobson, M.Z.: Climate response of fossil fuel and biofuel soot, accounting for soot's feedback to snow and sea ice albedo and emissivity. J. Geophys. Res. **109**, D21201 (2004). doi:10.1029/2004JD004945

Li, G., Zhang, R., Fan, J., Tie, X.: Impacts of black carbon aerosol on photolysis frequencies and ozone in the houston area. J. Geophys. Res. **110**, D23206 (2005). doi:10.1029/2005JD005898

McConnel, J., et al.: 20th-century industrial black carbon emissions altered arctic climate forcing. Science **317**, 1381–1384 (2007)

Park, R., Jacob, D.J., Kumar, N., Yantosca, R.M.: Regional visibility statistics in the United States: natural and transboundary pollution influences, and implications for the Regional Haze Rule. Atmos. Environ. **40**, 5405–5423 (2006). doi:10.1016/j.atmosenv.2006.04.059

Putaud, J.-P., Raes, F., Dingenen, R.V., et al.: A European aerosol phenomenology—2: chemical characteristics of particulate matter at kerbside, urban, rural and background sites in Europe. Atmos. Environ. **38**, 2579–2595 (2004)

Ramanathan, V., Carmichael, G.: Global and regional climate changes due to black carbon. Nat. Geosci. **1**, 221–227 (2008)

Ruellan, S., Cachier, H.: Characterisation of fresh particulate vehicular exhausts near a Paris high flow road. Atmos. Environ. **35**, 453–468 (2001)

Safai, P.D., Kewat, S., Praveen, P.S., Rao, P.S.P., Momin, G.A., Ali, K., Devara, P.C.S.: Seasonal variation of black carbon aerosols over a tropical urban city of Pune, India. Atmos. Environ. **41**, 2699–2709 (2007)

Streets, D.G., Bond, T.C., Carmichael, G.R., Fernandes, S.D., Fu, Q., He, D., Klimont, Z., Nelson, S.M., Tsai, N.Y., Wang, M.Q., Woo, J.H., Yarber, K.F.: An inventory of gaseous and primary aerosol emissions in Asia in the year 2000. J. Geophys. Res. **108**, 8809 (2003)

Tang, J., Wen, Y.O., Zhou, L.X.: Observational study of black carbon in clean air area of Western China. Q. J. Appl. Meteorol. **10**(2), 160–170 (1999). In Chinese

Tie, X., Cao, J.: Aerosol pollutions in eastern china; present and future impacts on environment. Particuology **7**, 426–431 (2009)

Tie, X., Geng, F.H., Peng, L., Gao, W., Zhao, C.S.: Measurement and modeling of O_3 variability in Shanghai, China; application of the WRF-Chem model. Atmos. Environ. **43**, 4289–4302 (2009)

Tripathi, S.N., Dey, S., Tare, V., Satheesh, S.K.: Aerosol black carbon radiative forcing at an industrial city in northern India. Geophys. Res. Lett. **32**, L08802 (2005). doi:10.1029/2005GL022515

Warren, S., Wiscombe, W.: A model for the spectral albedo of snow. II: snow containing atmospheric aerosols. J. Atmos. Sci. **37**, 2734–2745 (1980)

Watson, J.G., Chow, J.G., Chen, L.W.: Summary of organic and elemental carbon/black carbon analysis methods and intercomparisons. Aerosol Air Qual. Res. **5**, 65–102 (2005)

Wolff, E.W., Cachier, H.: Concentrations and seasonal cycle of black carbon in aerosol at a coastal Antarctic station. J. Geophys. Res. **103**, 11033–11041 (1998)

Xu, B.Q., Cao, J.J., Hansen, J., Yao, T.D., Joswia, D.R., Wang, N.L., Wu, G.J., Wang, M., Zhao, H. B., Yang, W., Liu, X.Q., He, J.Q.: Black soot and the survival of Tibetan glaciers. PNAS **106**, 22114–22118 (2009)